IEICE TRANS. COMMUN., VOL.E95–B, NO.3 MARCH 2012

PAPER

Iterative Superimposed Pilot-Assisted Channel Estimation Using Sliding Wiener Filtering for Single-Carrier Block Transmission

Tetsuya UCHIUMI[†a)], **Tatsunori OBARA**[†], **Kazuki TAKEDA**[†], ***Student Members***, ***and*** **Fumiyuki ADACHI**[†], ***Fellow***

SUMMARY In the conventional iterative superimposed pilot-assisted channel estimation (SI-PACE), simple averaging of the instantaneous channel estimates obtained by using the pilot over several single-carrier (SC) blocks (called the frame in this paper) is taken in order to reduce the interference from data symbols. Therefore, the conventional SI-PACE has low tracking ability against fading time variations. To solve the tracking problem, Wiener filtering (WF)-based averaging can be used instead of simple averaging. However, WF incurs high computational complexity. Furthermore, the estimation error of the fading autocorrelation function significantly degrades the channel estimation accuracy. In order to improve the channel estimation accuracy while keeping the computational complexity low, a new iterative SI-PACE using sliding WF (called iterative SWFSI-PACE) is proposed. The channel estimation is done by sliding a WF having a shorter filter size than the measurement interval. The bit error rate (BER) and throughput performances of SC-FDE using iterative SWFSI-PACE are investigated by computer simulation to show that the proposed scheme achieves good BER and throughput performances while keeping the computational complexity low irrespective of the fading rate (or maximum Doppler frequency).
key words: *superimposed pilot, Wiener filter, autocorrelation function estimation*

1. Introduction

In the next generation mobile communications systems, broadband services will be in greatly demand [1]. However, for such high-speed data transmissions, the wireless channel becomes severely frequency-selective and the bit error rate (BER) performance significantly degrades due to a large inter-symbol interference (ISI) [2].

Recently, single-carrier (SC) transmission with frequency-domain equalization (FDE) has been adopted as the uplink (mobile-to-base) transmission since it has low peak-to-average power ratio (PAPR) property and can take advantage of the channel severe frequency-selectivity by the use of FDE to improve the transmission performance [3], [4].

FDE requires accurate channel estimation. A well known channel estimation scheme is a pilot-assisted channel estimation (PACE) [5]–[9], in which the known pilot symbols are orthogonally multiplexed with data symbols in either time- or frequency-domain. However, this reduces the spectrum efficiency. On the other hand, a superimposed pilot-assisted channel estimation (SI-PACE) [7]–[9] allows a simultaneous transmission of pilot and data streams in parallel (see Fig. 1) and therefore, the spectrum efficiency is not reduced.

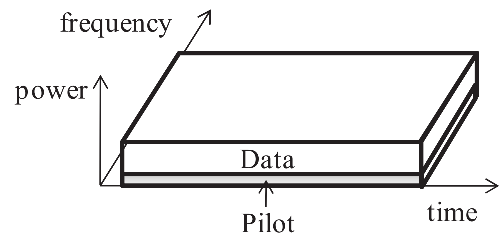

Fig. 1 Superimposed pilot.

In SI-PACE, the interference from the data stream degrades the channel estimation accuracy. To reduce the interference, simple averaging can be applied to the instantaneous channel estimates obtained by using pilot over a certain interval of SC blocks (called the frame in this paper) [8], [9]. However, the use of simple averaging results in lower tracking ability against fast fading.

To solve the tracking problem, Wiener filtering (WF) [10] can be introduced instead of simple averaging. However, the WF requires high computational complexity. It also requires knowledge of fading autocorrelation function. In order to improve the channel estimation accuracy while keeping the computational complexity low, we propose a new iterative SI-PACE using sliding WF-based averaging (called iterative SWFSI-PACE). In the proposed scheme, the channel estimation is done by sliding a WF that is shorter than the channel estimation interval. The channel estimation and data decision are iterated a sufficient number of times to further improve the accuracies of channel estimation and data detection.

The rest of paper is organized as follows. The signal transmission model is introduced in Sect. 2. The iterative SWFSI-PACE and MMSE-FDE are described in Sect. 3. In Sect. 4, the results of BER and throughput performance simulations are presented. Section 5 concludes this paper.

2. Signal Transmission Model

2.1 Transmit Signal Representation

The transmitter structure of SC with superimposed pilot is illustrated in Fig. 2. Throughout the paper, an equivalent low pass representation of discrete time signal is used and

Manuscript received April 13, 2011.
Manuscript revised October 24, 2011.
[†]The authors are with the Department of Electrical and Communication Engineering, Graduate School of Engineering, Tohoku University, Sendai-shi, 980-8579 Japan.
a) E-mail: uchiumi@mobile.ecei.tohoku.ac.jp
DOI: 10.1587/transcom.E95.B.924

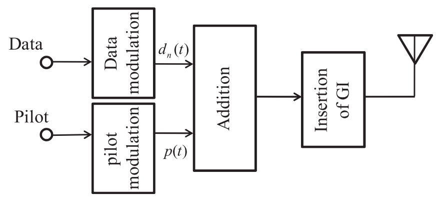

Fig. 2 Transmitter structure.

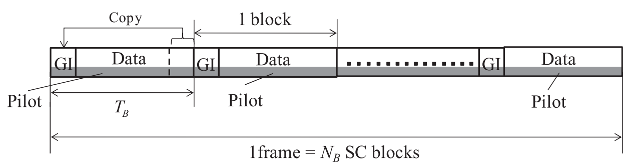

Fig. 3 Frame structure.

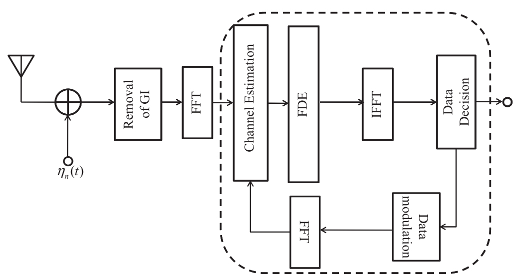

Fig. 4 Receiver structure of SC with iterative SWFSI-PACE.

T_s denotes symbol duration. At the transmitter, the block length is equal to the block size of fast Fourier transform (FFT) at the receiver for MMSE-FDE. The data symbol sequence in the $n(= 0 \sim N_B - 1)$th block is represented by $\{d_n(t); t = 0 \sim N_c - 1\}$ with $E[|d_n(t)|^2] = 1$. A pilot sequence $\{p(t); t = 0 \sim N_c - 1\}$ with $E[|p(t)|^2] = 1$ of N_c symbols superimposed to $\{d_n(t); t = 0 \sim N_c - 1\}$ to make a pilot-superimposed block.

The last N_g samples in each pilot-superimposed block of N_c samples is copied as the cyclic prefix and inserted into the guard interval (GI) at the beginning of each block. The nth pilot-superimposed block $\{s_n(t); t = -N_g \sim N_c - 1\}$ is represented as

$$s_n(t) = \sqrt{2P_D} d_n(t \bmod N_c) + \sqrt{2P_P} p(t \bmod N_c), \quad (1)$$

where P_D and P_P denote the signal power and pilot power, respectively. N_B blocks form a frame over which the channel estimation and data decision are done (see Fig. 3).

2.2 Received Signal Representation

The receiver structure of SC with iterative SWFSI-PACE is presented in Fig. 4. The propagation channel is assumed to be a frequency-selective fading channel having symbol-spaced L discrete paths, each subjected to independent fading. The channel impulse response associated with the nth block is expressed as

$$h_n(\tau) = \sum_{l=0}^{L-1} h_{n,l}\delta(\tau - \tau_l), \quad (2)$$

with $E\left[\sum_{l=0}^{L-1} |h_l|^2\right] = 1$ ($E[.]$ denotes the ensemble average operation) where $h_{n,l}$ and τ_l denote complex-valued path gain and time delay of the lth path ($l = 0 \sim L - 1$) in the tth time, respectively. The maximum time delay τ_{L-1} is assumed to be shorter than GI length.

After GI removal, the received nth block $\{y_n(t); t = 0 \sim N_c - 1\}$ can be expressed as

$$y_n(t) = \sum_{l=0}^{L-1} h_{n,l} s_n((t - \tau_l) \bmod N_c) + \eta_n(t), \quad (3)$$

where $\eta_n(t)$ denotes a zero-mean complex-valued Gaussian variable having variance $E[|\eta_n(t)|^2] = 2N_0/T_s$ (where N_0 is the power spectrum density of the additive white Gaussian noise (AWGN)).

The received block is transformed by N_c-point FFT into the frequency-domain signal $\{Y_n(k); k = 0 \sim N_c - 1\}$. $Y_n(k)$ is given as

$$Y_n(k) = \left\{\sqrt{2P_D} D_n(k) + \sqrt{2P_P} P(k)\right\} H_n(k) + N_n(k), \quad (4)$$

where $H_n(k)$ and $N_n(k)$ denote the channel gain and channel noise at the kth frequency, respectively. $H_n(k)$, $N_n(k)$, $D_n(k)$, and $P_n(k)$ are given by

$$\begin{cases} H_n(k) = \sum_{l=0}^{L-1} h_{n,l} \exp\left(-j2\pi \frac{\tau_l}{N_c} k\right) \\ N_n(k) = \frac{1}{\sqrt{N_c}} \sum_{t=0}^{N_c-1} \eta_n(t) \exp\left(-j2\pi \frac{t}{N_c} k\right) \\ D_n(k) = \frac{1}{\sqrt{N_c}} \sum_{t=0}^{N_c-1} d_n(t) \exp\left(-j2\pi \frac{t}{N_c} k\right) \\ P(k) = \frac{1}{\sqrt{N_c}} \sum_{t=0}^{N_c-1} p(t) \exp\left(-j2\pi \frac{t}{N_c} k\right). \end{cases} \quad (5)$$

3. Iterative SWFSI-PACE and MMSE-FDE

In the conventional iterative SI-PACE [8], [9], since the simple averaging is used to reduce the interference from data stream, the conventional SI-PACE has low tracking ability against fading. To solve this tracking problem, Wiener filtering (WF) can be introduced instead of simple averaging. However, the channel estimation using WF of a large filter size (equal to the frame of N_B blocks) has two problems: high computational complexity and low estimation accuracy of autocorrelation function which is necessary to construct the WF. To solve the problems, we propose to estimate the channel by sliding a WF having a short filter size of N_T ($\leq N_B$) blocks, as shown in Fig. 5. For constructing the WF of a short filter size, the time difference range of the autocorrelation function can be shortened and therefore, sufficiently accurate channel estimation is possible since a

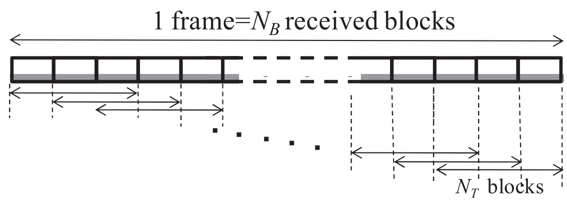

Fig. 5 Proposed sliding WF-based channel estimation.

sufficient number of samples can be involved to estimate the autocorrelation function. In addition to this, the computational complexity required for matrix inversion can be much reduced since a number of complex multiply and addition operations required for matrix inversion is in an order of $O(N_{N_T}^3)$.

The channel estimate at the ith iteration stage is denoted by $\left\{\hat{H}_n^{(i)}(k); k = 0 \sim N_c - 1\right\}$, $n = 0 \sim N_B - 1$. The number of iterations is denoted by I. At the initial iteration stage ($i = 0$), the channel estimation is done by using the superimposed pilot only. In the 1st stage onward ($i > 0$), the tentative data decisions obtained by the previous stage over a frame are fedback as an additional pilot.

3.1 Initial Stage ($i = 0$)

The WF requires the knowledge of the channel autocorrelation vector $\mathbf{A}_n$ of size $1 \times N_T$ and the channel autocorrelation matrix $\mathbf{R}$ of size $N_T \times N_T$. $\mathbf{A}_n$ and $\mathbf{R}$ are defined as

$$\begin{cases} \mathbf{A}_n = E[H_n(k)\mathbf{H}(k)] \\ \quad = [R(N_T-1)/2, \ldots, R(0), \ldots, R(N_T-1)] \\ \mathbf{R} = E\left[\mathbf{H}(k)\mathbf{H}^H(k)\right] \\ \quad = \begin{bmatrix} R(0) & R(1) & \ldots & R(N_T-1) \\ R(1) & R(0) & & \vdots \\ \vdots & & \ddots & R(1) \\ R(N_T-1) & \ldots & R(1) & R(N_T-1) \end{bmatrix}, \end{cases} \tag{6}$$

where $\mathbf{H} = [H_{n-(N_T-1)/2}(k), \ldots, H_{n+(N_T-1)/2}(k)]^T$, $R(m) = E[H_n(k)H_{n+m}^*(k)]$, $m = 0 \sim N_T - 1$, and $(.)^H$ denotes the Hermitian conjugate operation. The autocorrelation function $R(m)$ is estimated by the simple averaging as

$$R^{(-1)}(m) = \frac{\sum_{k=0}^{N_c-1}\sum_{n=0}^{N_B-1-m} \hat{H}_n^{(-1)}(k)\hat{H}_{n+m}^{(-1)*}(k)}{\sum_{k=0}^{N_c-1}\sum_{n=0}^{N_B-1-m} \left|\hat{H}_n^{(-1)}(k)\right|^2}, \tag{7}$$

where $\hat{H}_n^{(-1)}(k)$ is the estimate of $H_n(k)$ obtained by using the superimposed pilot only and the delay time-domain windowing technique [5], given as

$$\hat{H}_n^{(-1)}(k) = \frac{1}{\sqrt{N_c}}\sum_{\tau=0}^{N_c-1} w(\tau)\hat{h}_n^{(-1)}(\tau)\exp\left(-j2\pi\frac{\tau}{N_c}k\right), \tag{8}$$

with

$$\begin{cases} \tilde{H}_n^{(-1)}(k) = \dfrac{Y_n(k)}{\sqrt{2P_P}P(k)} \\ \hat{h}_n^{(-1)}(\tau) = \dfrac{1}{\sqrt{N_c}}\sum_{k=0}^{N_c-1} \tilde{H}_n^{(-1)}(k)\exp\left(j2\pi\dfrac{\tau}{N_c}k\right) \\ w(\tau) = \begin{cases} 1, & 0 \le \tau \le N_g - 1 \\ 0, & \text{otherwise} \end{cases} . \end{cases} \tag{9}$$

As understood from Eq. (7), the number of samples which are used for estimating the autocorrelation function $R(m)$, $m = 0 \sim N_T - 1$, is given by $N_B - m$. For SI-PACE using frame-size WF (i.e., $N_T = N_B$), the number of available samples for estimating $R(m)$ decreases as m approaches $N_T - 1$, resulting in the degraded estimation accuracy. However, for SI-PACE using sliding WF (i.e., N_T is much smaller than N_B), a sufficient number of samples for estimating $R(m)$ is obtained over an entire range of $m = 0 \sim N_T - 1$ and hence, a good estimation accuracy is achieved.

Then, sliding WF channel estimation is applied to obtain the improved channel estimate $\hat{H}_n^{(0)}(k)$ as

$$\tilde{H}_n^{(0)}(k) = \mathbf{W}_n^{(0)}(k)\mathbf{Y}(k), \tag{10}$$

where $\mathbf{Y}(k) = \left[Y_{n-(N_T-1)/2}(k), \ldots, Y_{n+(N_T-1)/2}(k)\right]^T$ is the received symbol vector of size $N_T \times 1$ and $\mathbf{W}_n^{(0)}(k) = \left[W_{n,0}^{(0)}(k), \ldots, W_{n,N_T-1}^{(0)}(k)\right]$ is the WF weight of size $1 \times N_T$. $\mathbf{W}_n^{(0)}(k)$ is given, from [10], as

$$\mathbf{W}_n^{(0)}(k) = \mathbf{A}_n^{(-1)}\mathbf{P}^H(k) \times \left[\mathbf{P}(k)\mathbf{R}^{(-1)}\mathbf{P}^H(k) + \mathbf{\Lambda}_N^{(-1)}\right]^{-1}, \tag{11}$$

where $\mathbf{P}(k) = \sqrt{2P_P}P(k)\mathbf{I}$ is the pilot matrix of size $N_T \times N_T$. $\mathbf{A}_n^{(-1)}$ and $\mathbf{R}^{(-1)}$ are estimates of $\mathbf{A}_n$ and $\mathbf{R}$, respectively, and are given by Eq. (6) with replacing $R(m)$ by $R^{-1}(m)$. In Eq. (11), $\mathbf{\Lambda}_N^{(-1)} = diag\left[2\hat{P}_0^{(-1)}, \ldots, 2\hat{P}_{N_B-1}^{(-1)}\right]$ is an estimate of the noise covariance matrix $\mathbf{\Lambda}_N = 2P\mathbf{I}$ of size $N_T \times N_T$, where $\hat{P}_n^{(-1)}$ is the estimate of the noise plus signal power and is obtained as

$$\hat{P}_n^{(-1)} = \frac{1}{N_B N_c}\sum_{j=0}^{N_B-1}\sum_{k=0}^{N_c-1}\left|Y_j(k) - \sqrt{2P_P}P(k)\hat{H}_j^{(-1)}(k)\right|^2. \tag{12}$$

In the initial stage, the data signal component is unknown and cannot be removed from the received signal. Therefore, the noise plus signal power is estimated instead of the noise power as shown in Eq. (12). Again, the delay time-domain windowing technique [5] is applied to obtain the improved channel estimate as

$$\hat{H}_n^{(0)}(k) = \frac{1}{\sqrt{N_c}}\sum_{\tau=0}^{N_c-1} w(\tau)\hat{h}_n^{(0)}(\tau)\exp\left(-j2\pi\frac{\tau}{N_c}k\right), \tag{13}$$

with

$$\begin{cases} \hat{h}_n^{(0)}(\tau) = \dfrac{1}{\sqrt{N_c}} \displaystyle\sum_{k=0}^{N_c-1} \tilde{H}_n^{(0)}(k) \exp\left(j2\pi \frac{\tau}{N_c} k\right) \\ w(\tau) = \begin{cases} 1, & 0 \le \tau \le N_g - 1 \\ 0, & \text{otherwise} \end{cases} \end{cases} . \tag{14}$$

Finally, the frequency-domain signal estimate $\{\hat{D}_n^{(0)}(k); k = 0 \sim N_c - 1\}$ is obtained as

$$\hat{D}_n^{(0)}(k) = M_n^{(0)}(k) \left\{ Y_n(k) - \sqrt{2P_P} \hat{H}_n^{(0)}(k) P(k) \right\}, \tag{15}$$

where $M_n^{(0)}(k)$ is the MMSE weight [5], given by

$$M_n^{(0)}(k) = \frac{\hat{H}_n^{(0)*}(k)}{\left|\hat{H}_n^{(0)}(k)\right|^2 + \hat{P}_n^{(0)} / P_D}, \tag{16}$$

where $\hat{P}_n^{(0)}$ is obtained using Eq. (12) with replacing $\hat{H}_j^{(-1)}(k)$ by $\hat{H}_j^{(0)}(k)$. In this paper, it is assumed that the receiver has a perfect knowledge of P_D and P_P.

After joint MMSE-FDE and pilot cancellation, the time-domain soft-decision symbol block $\{\hat{d}_n^{(0)}(t); t = 0 \sim N_c - 1\}$ is obtained by applying IFFT as

$$\hat{d}_n^{(0)}(t) = \frac{1}{\sqrt{N_c}} \sum_{k=0}^{N_c-1} \hat{D}_n^{(0)}(k) \exp\left(j2\pi \frac{t}{N_c} k\right), \tag{17}$$

from which the tentative data symbol decision is carried out to generate the data symbol block replica $\{\bar{d}_n^{(0)}(t); t = 0 \sim N_c - 1\}$ which is fed back to be used in the next iteration stage as an additional pilot.

3.2 $i(\ge 1)$th Stage

In the ith iteration stage, the channel estimate $\hat{H}_n^{(i-1)}(k)$ obtained in the previous iteration stage is used to estimate the autocorrelation function. Then, sliding WF channel estimation with the delay time-domain windowing technique [5] is done by using both the superimposed pilot and the symbol block replica $\{\bar{d}_n^{(i-1)}(t); t = 0 \sim N_c - 1\}$ generated by feeding back the decision made in the previous iteration stage as

$$\hat{H}_n^{(i)}(k) = \frac{1}{\sqrt{N_c}} \sum_{\tau=0}^{N_c-1} w(\tau) \hat{h}_n^{(i)}(\tau) \exp\left(-j2\pi \frac{\tau}{N_c} k\right), \tag{18}$$

with

$$\begin{cases} \tilde{H}_n^{(i)}(k) = \mathbf{W}_n^{(i)}(k) \mathbf{Y}(k) \\ \hat{h}_n^{(i)}(\tau) = \dfrac{1}{\sqrt{N_c}} \displaystyle\sum_{k=0}^{N_c-1} \tilde{H}_n^{(i)}(k) \exp\left(j2\pi \frac{\tau}{N_c} k\right) \\ w(\tau) = \begin{cases} 1, & 0 \le \tau \le N_g - 1 \\ 0, & \text{otherwise} \end{cases} \end{cases} , \tag{19}$$

where $\mathbf{Y}(k) = [Y_{n-(N_T-1)/2}(k), \ldots, Y_{n+(N_T-1)/2}(k)]^T$ and $\mathbf{W}_n^{(i)}(k) = \left[W_{n,0}^{(0)}(k), \ldots, W_{n,N_T-1}^{(0)}(k)\right]$. $\mathbf{W}_n^{(i)}(k)$ is given by

$$\mathbf{W}_n^{(i)}(k) = \mathbf{A}_n^{(i-1)} \left[\bar{\mathbf{D}}^{(i-1)H}(k) + \mathbf{P}^H(k)\right] \times \begin{bmatrix} \left(\bar{\mathbf{D}}^{(i-1)H}(k) + \mathbf{P}(k)\right) \mathbf{R}^{(-1)} \\ \times \left(\bar{\mathbf{D}}^{(i-1)H}(k) + \mathbf{P}^H(k)\right) + \mathbf{\Lambda}_N^{(i-1)} \end{bmatrix}^{-1}, \tag{20}$$

with

$$\begin{cases} \bar{\mathbf{D}}^{(i-1)}(k) \\ = \sqrt{2P_D} diag\left[\bar{D}_{n-(N_T-1)/2}^{(i-1)}(k), \ldots, \bar{D}_{n+(N_T-1)/2}^{(i-1)}(k)\right] \\ \mathbf{\Lambda}_n^{(i-1)} = diag\left[2\hat{P}_{n-(N_T-1)/2}^{(i-1)}, \ldots, 2\hat{P}_{n+(N_T-1)/2}^{(i-1)}\right], \end{cases} \tag{21}$$

where $\left\{\bar{D}_n^{(i-1)}(k); k = 0 \sim N_c - 1\right\}$ is the frequency-domain signal of the nth block data symbol sequence replica and $\hat{P}_n^{(i-1)}$ is obtained as

$$\hat{P}_n^{(i-1)} = \frac{1}{N_c} \sum_{k=0}^{N_c-1} \left| \begin{matrix} Y_n(k) - \hat{H}_n^{(i-1)}(k) \\ \times \left\{ \sqrt{2P_D} \bar{D}_n^{(i-1)}(k) + \sqrt{2P_P} P(k) \right\} \end{matrix} \right|^2 . \tag{22}$$

$\mathbf{A}_n^{(i-1)}$ and $\mathbf{R}^{(i-1)}$ are estimates of $\mathbf{A}_n$ and $\mathbf{R}$, respectively, and are given by Eq. (6) with replacing $R(m)$ by $R^{(i-1)}(m)$. $R^{(i-1)}(m)$ is obtained using Eq. (7) with replacing $\hat{H}_n^{(-1)}(k)$ by $\hat{H}_n^{(i-1)}(k)$.

Finally, the frequency-domain signal estimate $\{\bar{D}_n^{(i)}(k); k = 0 \sim N_c - 1\}$ is obtained as

$$\hat{D}_n^{(i)}(k) = M_n^{(i)}(k) \left\{ Y_n(k) - \sqrt{2P_P} \hat{H}_n^{(i)}(k) P(k) \right\}, \tag{23}$$

where $M_n^{(i)}(k)$ is the MMSE weight generated using Eq. (16) with replacing $\hat{H}_n^{(0)}(k)$ and $\hat{P}_n^{(0)}$ by $\hat{H}_n^{(i)}(k)$ and $\hat{P}_n^{(i)}$, respectively (note that $\hat{P}_n^{(i)}$ is obtained using Eq. (22) with replacing $\hat{H}_n^{(i-1)}(k)$ by $\hat{H}_n^{(i)}(k)$).

After joint MMSE-FDE and pilot cancellation, the time-domain soft-decision symbol block $\{\hat{d}_n^{(i)}(t); t = 0 \sim N_c - 1\}$ is obtained by applying IFFT as in Eq. (17). Then, the data symbol block replica $\{\bar{d}_n^{(i)}(t); t = 0 \sim N_c - 1\}$ is generated and fed back to be used in the $(i+1)$th iteration stage as an additional pilot.

3.3 Complexity

The number of complex multiply and addition operations required for iterative SWFSI-PACE is shown in Table 1, where I denotes the number of iterations. The Gaussian elimination method for matrix inversion is used. The number of complex multiply and addition operations is taken from [13].

The number of complex multiply and addition operations is plotted as a function of the filter N_T in Fig. 6. It can be seen from Fig. 6 that the number of complex multiply and addition operations can be reduced by choosing a

Table 1 No. of complex multiply and addition operations.

		No. of complex multiply operations	No. of complex addition operations
Wiener filter construction	Matrix inversion	$I\times N_c\times N_B\times (2N_T^3+6N_T^2-3N_T)/6$	$I\times N_c\times N_B\times (2N_T^3+3N_T^2-5N_T)/6$
	Matrix multiplication	$I\times N_c\times N_B\times (2N_T^3+2N_T^2)$	$I\times N_c\times N_B\times \{2N_T^2(N_T-1)+N_T^2-2N_T(N_T-1)\}$
Channel estimation using Wiener filter		$I\times N_c\times N_B\times N_T$	$I\times N_c\times N_B\times (N_T-1)$
Total		$I\times N_c\times N_B\times (14N_T^3+18N_T^2+3N_T)/6$	$I\times N_c\times N_B\times (14N_T^3+9N_T^2-5N_T-12)/6$

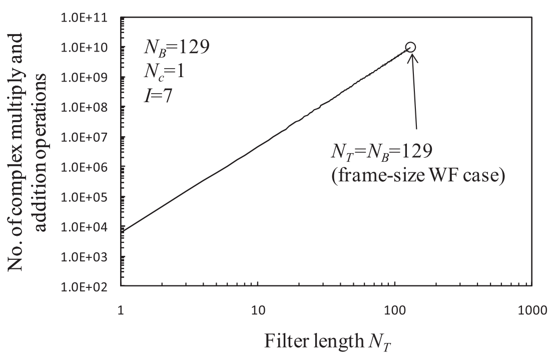

Fig. 6 No. of complex multiply and addition operations when $N_B = 129$, $N_c = 1$, and $I = 7$.

sufficiently small filter size N_T. For example, when $N_T = 9$ and $N_B = 129$, the number of complex multiply and addition operations can be reduced to about 0.03% of the case of frame-size WF ($N_T = N_B = 129$). However, if too short filter size is used, the accuracy of channel estimation degrades due to the reduced pilot power. Therefore, there exists the optimal filter size which will be found by computer simulation in Sect. 4.

4. Computer Simulation

Simulation parameters are summarized in Table 2. Quaternary phase shift keying (QPSK) data modulation, FFT block size of $N_c = 512$ and GI length of $N_g = 64$ symbols are assumed. Chu sequence [11] is used as the pilot. The propagation channel is assumed to be a symbol-spaced L=16-path frequency-selective Rayleigh fading channel; each path is generated by Jakes model [2]. Ideal sampling timing at the receiver is also assumed. The pilot power-to-data power ratio β and N_T are optimized by computer simulation.

4.1 Parameter Optimization

First, the frame size N_B is optimized for the conventional iterative SI-PACE using the flame-size WF. Figure 7 plots the mean square error (MSE) of the channel estimation using the flame-size WF as a function of N_B, where MSE is defined as $MSE = (1/N_cN_B)\sum_{n=0}^{N_B-1}\sum_{k=0}^{N_c-1}\left|H_n(k)-\hat{H}_n^{(I)}(k)\right|^2$, for $\beta = 1/32$ and $I = 11$ (the number of iterations) when the normalized maximum Doppler frequency $f_DT_s =$

Table 2 Simulation condition.

Transmitter	Modulation	QPSK
	No. of FFT points	N_c=512
	GI	N_g=64
	Pilot sequence	Chu sequence
Channel	Fading	Frequency –selective Rayleigh fading
	Power delay profile	L=16-path uniform power delay profile
	Delay time	τ_l=l
Receiver	Frequency-domain Equalization	MMSE
	Channel Estimation	Iterative SWFSI-PACE
	Autocorrelation matrix	estimation

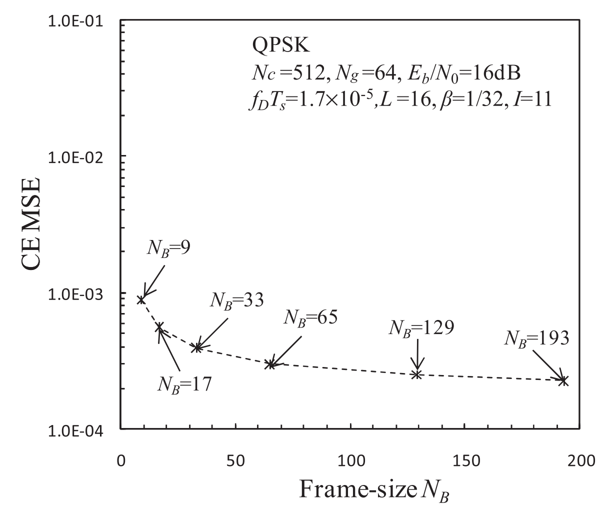

Fig. 7 Impact of frame size N_B on achievable MSE ($I = 11$).

1.74×10^{-5} (this corresponds to a mobile terminal moving speed of 375km/h for symbol rate $1/T_s$ of 100 Msps and a carrier frequency of 5 GHz) and the average received bit energy-to-AWGN noise power spectrum density ratio $E_b/N_0 = 0.5(1+N_g/N_c)(E_s/N_0)(\beta+1) = 16$ dB. It can be seen from Fig. 7 that, as N_B increases, the MSE performance improves. However, the computational complexity of the proposed SI-PACE using sliding WF becomes higher. Considering a trade-off between the performance and the complexity, the frame size of $N_B = 129$ is used in this paper.

Next, the filter size N_T and pilot power-to-data power ratio β are optimized for the proposed iterative SWFSI-PACE. Figure 8 plots the average BER performance of the proposed channel estimation with $I = 11$ as a function of β with N_T as a parameter when $f_DT_s = 1.74\times10^{-5}(1.74\times10^{-7})$ and $E_b/N_0 = 16$ dB. It can be seen from Fig. 8 that the use of too small or too large β (or N_T) degrades the achievable BER performance. The reason for this is that, when β (or N_T) is too small, enough pilot power cannot be obtained and when β is too large, the data power loss due to the pilot is big. When N_T is too large, the tracking ability against fading tends to be lost. The use of N_T=9(33) and β=1/32(1/64) is found to provide the best BER performance when $f_DT_s = 1.74\times10^{-5}$ (1.74×10^{-7}).

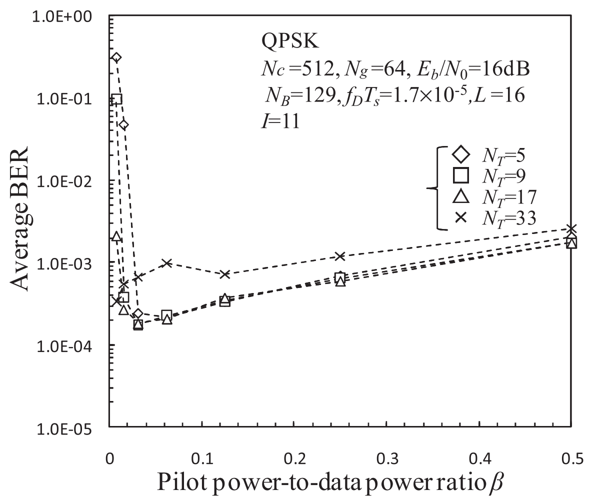

(a) $f_D T_s = 1.74 \times 10^{-5}$

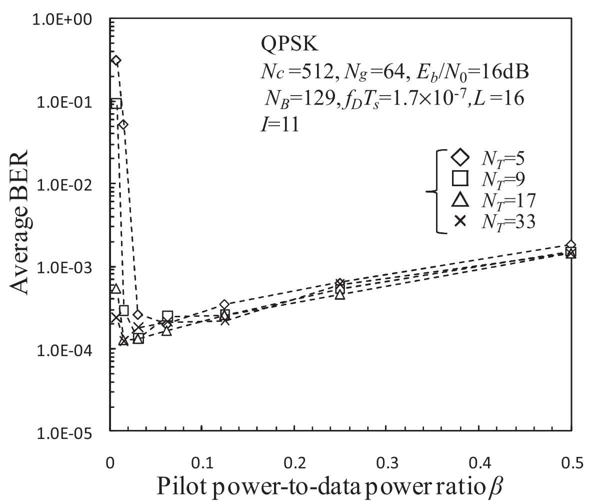

(b) $f_D T_s = 1.74 \times 10^{-7}$

Fig. 8 Effect of pilot power-to-data power ratio β and filter size N_T on achievable BER ($I = 11$).

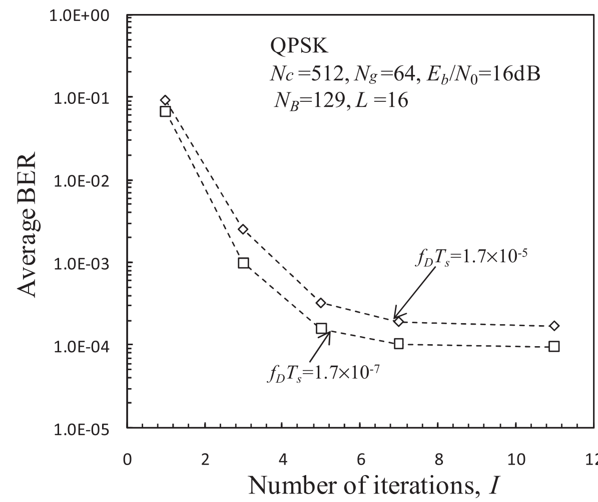

Fig. 9 Effect of number of iterations, I, on achievable BER.

Figure 9 plots the BER performance as a function of the number I of iterations with $N_T = 9(33)$ and $\beta = 1/32(1/64)$ when $f_D T_s = 1.74 \times 10^{-5}(1.74 \times 10^{-7})$. It can be seen from Fig. 9 that the use of $I = 11$ provides a sufficiently improved BER performance. When $N_T = 9$, the computational complexity of CE can be reduced to 0.03% compared to frame-size WF (i.e., $N_B = N_T$). In the following simulation, $N_T = 9(33)$ and $\beta = 1/32(1/64)$ are used when $f_D T_s = 1.74 \times 10^{-5}(1.74 \times 10^{-7})$.

4.2 BER Performance

Figure 10 plots the BER performance achievable with the proposed iterative SWFSI-PACE when $f_D T_s = 1.74 \times 10^{-5}$ (1.74×10^{-7}). For comparison, also plotted are the BER performances achievable with the conventional iterative SI-PACE using the flame-size WF ($N_T = 129$) and the simple averaging. The autocorrelation function is estimated by using Eq. (23). It can be seen from Fig. 10 that when $f_D T_s =$

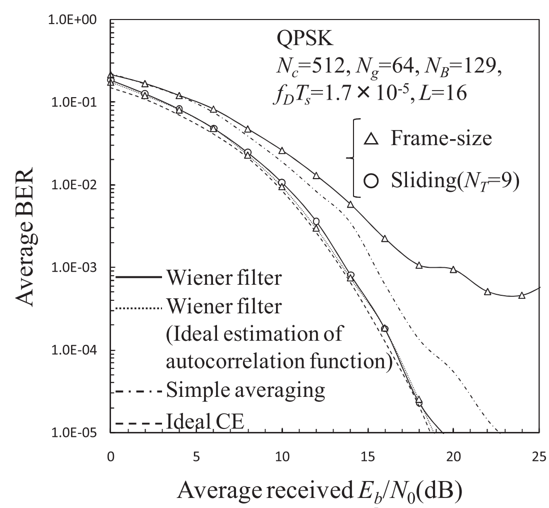

(a) $f_D T_s = 1.74 \times 10^{-5}$

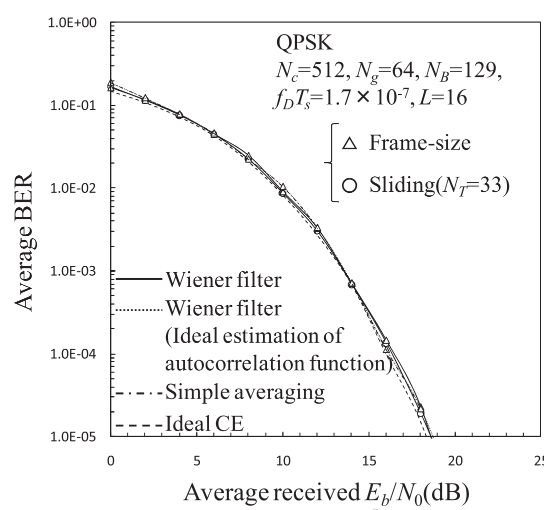

(b) $f_D T_s = 1.74 \times 10^{-7}$

Fig. 10 BER performance.

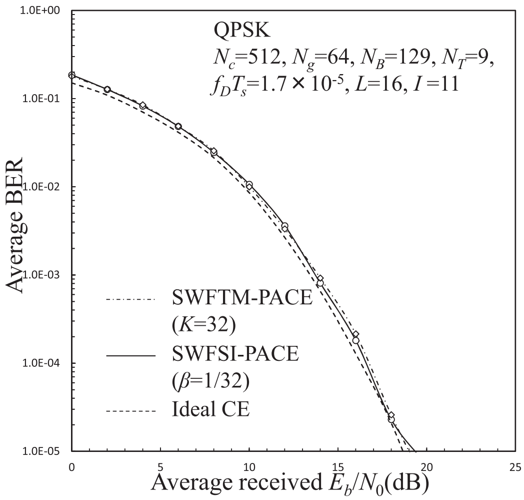

Fig. 11 BER comparison of SWFSI-PACE and SWFTM-PACE.

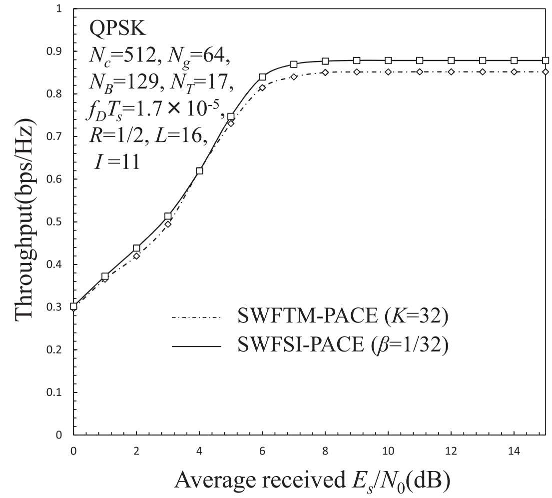

Fig. 12 Throughput performance comparison.

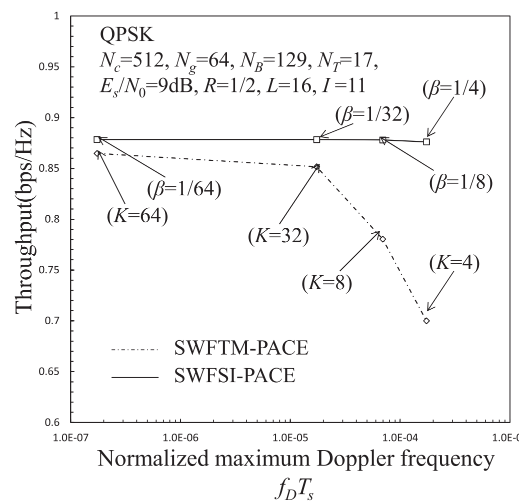

Fig. 13 Impact of fading rate on throughput.

$1.74{\times}10^{-7}$, the simple averaging, the frame-size WF, and the proposed channel estimation achieve almost the same performance. On the other hands, when $f_DT_s = 1.74{\times}10^{-5}$, the proposed channel estimation can achieve better BER performance than the conventional channel estimation. This reason is that, in the proposed channel estimation, even if fading channel is very fast, the sufficiently accurate estimation of autocorrelation function is possible since sufficient number of samples can be involved to estimate the autocorrelation function. It should be noted that the BER performance SI-PACE using simple averaging degrades compared to the proposed SI-PACE using sliding WF since the simple averaging has lower tracking ability against the fast fading.

4.3 Performance Comparison of Proposed SI-PACE and TM-PACE

The idea of iterative SWF can also be applied to the time-multiplexed (TM) pilot case. Figure 11 compares the BER performances of the proposed iterative SWFSI-PACE and a sliding WF based iterative TM-PACE (iterative SWFTM-PACE) when $f_DT_s = 1.74 \times 10^{-5}$. In the case of iterative SWFTM-PACE, the pilot block is assumed to be periodically transmitted every $K = 32$ blocks. It can be seen from Fig. 11 that the iterative SWFSI-PACE achieves almost the same BER performance as the iterative SWFTM-PACE.

4.4 Throughput Performance Comparison

The iterative SWFSI-PACE and iterative SWFTM-PACE are compared in terms of throughput when the hybrid automatic repeat request (HARQ) [14], [15] using selective repeat (SR) strategy [17] is used. In the SR strategy, error information of each block is fed back to the transmitter. If there is any erroneously received block in a frame, the same block is retransmitted, otherwise a new block is transmitted. Chase combining is used as packet combining [15], [16]. In this paper, ideal error detection and ideal feedback channel are assumed. As a channel coding, a turbo coding is assumed with an encoder with two (13,15) RSC encoders (coding rate $R = 1/2$) and a decoder with Log-MAP algorithm.

Figure 12 plots the throughput performance of iterative SWFSI-PACE and iterative SWFTM-PACE both with $I = 11$, $N_T = 17$, and $\beta = 1/32(K = 32)$ when $f_DT_s = 1.74 \times 10^{-5}$. It can be seen from Fig. 12 that both channel estimation schemes can achieve almost the same throughput performance. However, the throughput of the SWFSI-PACE is slightly higher than the SWFTM-PACE in a high E_s/N_0 region.

Figure 13 plots the throughput performance as a function of fDTs when $E_s/N_0 = 9$ dB. N_T, β, and K are optimized for each f_DT_s. It can be seen from Fig. 13 that the SWFSI-PACE achieves a higher throughput than SWFTM-PACE. As the fading rate increases, the throughput of SWFTM-PACE reduces since the pilot interval needs to be shorted in order to improve tracking ability.

5. Conclusion

In this paper, we proposed a new sliding WF-based iterative SI-PACE (iterative SWFSI-PACE). It was shown that iterative SWFSI-PACE can achieve a good BER performance with reduced computational complexity. The computational complexity can be reduced to about 0.03% of the frame-size WF based channel estimation. We also applied to the idea of sliding WF-based channel estimation to the time-multiplexed (TM) pilot case. It was shown that the both iterative SWFSI-PACE and iterative SWTM-PACE provide almost the same BER performance; however, the SWSI-PACE can achieve a slightly higher throughput in a high E_s/N_0 region and also under a fast fading environment.

References

[1] F. Adachi, "Wireless past and future-evolving mobile communications systems," IEICE Trans. Fundamentals, vol.E83-A, no.1, pp.55–60, Jan. 2001.
[2] J.G. Proalis, Digital communications, 4th ed., McGraw-Hill, 2001.
[3] F. Adachi, T. Sao, and T. Itagaki, "Performance of multicode DS-CDMA using frequency domain equalization in a frequency selective fading channel," Electron. Lett., vol.39, no.2, pp.239–241, Jan. 2003.
[4] D. Falconer, S.L. Ariyavisitakul, A. Benyamin-Seeyarand, and B. Edison, "Frequency domain equalization for single-carrier broadband wireless systems," IEEE Commun. Mag., vol.40, no.4, pp.58–66, April 2002.
[5] K. Takeda and F. Adachi, "SNR estimation for pilot-assisted frequency-domain MMSE channel estimation," Proc. IEEE VTS APWCS, Hokkaido University, Japan, Aug. 2005.
[6] C.-T. Lam, D. Falconer, F. Danilo-Lemoine, and R. Dinis, "Channel estimation for SC-FDE systems using frequency domain multiplexed pilots," Proc. IEEE VTC 2006, pp.1–5, Sept. 2006.
[7] P. Hoeher and F. Tufvesson, "Channel estimation with superimposed pilot sequence," Proc. IEEE GLOBECOM 99, vol.4, pp.2162–2166, Rio de Janeiro, Brazil, Dec. 1999.
[8] R. Dinis, N. Souto, J. Silva, A. Kumar, and A. Correia, "Joint detection and channel estimation for OFDM signals with implicit pilots," Proc. IEEE Mobile and Wireless Communications Summit, pp.1–5, Hungary, July 2007.
[9] M.M. da Silva, R. Dinis, and A.M.C. Correia, "Joint detection and channel estimation for SC-FDE with STBC," Proc. 15th Asia-Pacific Conference on Communications (APCC) Shanghai, pp.157–160, Oct. 2009.
[10] S. Haykin, Adaptive filter theory, 4th ed., Prentice Hall, 2002.
[11] D.C. Chu, "Polyphase codes with good periodic correlation properties," IEEE Trans. Inf. Theory, vol.18, no.4, pp.531–532, July 1972.
[12] C. Berrou, A. Glavieux, and P. Thitimajshima, "Near Shannon limit error-correcting codeing and decoding-turbo codes," Proc. IEEE ICC, pp.1064–1070, May 1993.
[13] R.W. Farebrother, Linear Least Squares Computations, Marcel Dekker, 1988.
[14] D. Garg and F. Adachi, "Throughput comparison of turbo-coded HARQ in OFDM, MC-CDMA and DS-CDMA with frequency domain equalization," IEICE Trans. Commun., vol.E88-B, no.2, pp.664–667, Feb. 2005.
[15] T. Yui, H. Tomeba, and F. Adachi, "Pilot-assisted adaptive channel estimation for coded MC-CDMA with ICI cancellation," IEICE Trans. Commun., vol.E92-B, no.1, pp.246–253, Jan. 2009.
[16] D. Chase, "Code combining-A maximum-likelihood decoding approach for combining an arbitrary number of noisy packets," IEEE Trans. Commun., vol.33, no.5, pp.385–393, May 1985.
[17] R.A. Comroe and D.J. Costello, "ARQ schemes for data transmission in mobile radio systems," IEEE J. Sel. Areas Commun., vol.2, no.4, pp.472–481, July 1984.

Tetsuya Uchiumi received his B.S. degrees in communications engineering from Tohoku University in 2009. Currently, he is a M.S. student in the Department of Electrical and Communications Engineering, Graduate School of Engineering, Tohoku University. His research interests include channel estimation for frequency-domain equalization in mobile communication systems.

Tatsunori Obara received his B.S. degree in Electrical, Information and Physics Engineering in 2008 and M.S. degree in communications engineering, in 2010, respectively, from Tohoku University, Sendai Japan. Currently he is a graduate student, studying toward his PhD degree at the Department of Electrical and Communications Engineering, Graduate School of Engineering, Tohoku University. His research interests include channel equalization techniques for mobile communication systems.

Kazuki Takeda received his B.S., M.S., and Dr. Eng. degrees in communications engineering from Tohoku University, Sendai, Japan, in 2006 and 2008, and 2010, respectively. Currently he is a Japan Society for the Promotion of Science (JSPS) research fellow at the Department of Electrical and Communications Engineering, Graduate School of Engineering, Tohoku University. His research interests include precoding and channel equalization techniques for mobile communication systems. He was a recipient of the 2009 IEICE RCS (Radio Communication Systems) Active Research Award.

Fumiyuki Adachi received the B.S. and Dr. Eng. degrees in electrical engineering from Tohoku University, Sendai, Japan, in 1973 and 1984, respectively. In April 1973, he joined the Electrical Communications Laboratories of Nippon Telegraph & Telephone Corporation (now NTT) and conducted various types of research related to digital cellular mobile communications. From July 1992 to December 1999, he was with NTT Mobile Communications Network, Inc. (now NTT DoCoMo, Inc.), where he led a research group on wideband/broadband CDMA wireless access for IMT-2000 and beyond. Since January 2000, he has been with Tohoku University, Sendai, Japan, where he is a Professor of Electrical and Communication Engineering at the Graduate School of Engineering. His research interests are in CDMA wireless access techniques, equalization, transmit/receive antenna diversity, MIMO, adaptive transmission, and channel coding, with particular application to broadband wireless communications systems. He is a program reader of the 5-year Global COE Program "Center of Education and Research for Information Electronics Systems" (2007–2011), awarded by the Ministry of Education, Culture, Sports, Science and Technology of Japan. From October 1984 to September 1985, he was a United Kingdom SERC Visiting Research Fellow in the Department of Electrical Engineering and Electronics at Liverpool University. He was a co-recipient of the IEICE Transactions best paper of the year award 1996, 1998 and 2009 and also a recipient of Achievement award 2003. He is an IEEE Fellow and was a co-recipient of the IEEE Vehicular Technology Transactions best paper of the year award 1980 and again 1990 and also a recipient of Avant Garde award 2000. He was a recipient of Thomson Scientific Research Front Award 2004 and Ericsson Telecommunications Award 2008, Telecom System Technology Award 2009, and Prime Minister Invention Prize 2010.